Dimensionless Parameters Characterizing Atmospheric Pollution in Valley

Akira KONDO

Graduate School of Engineering, Osaka University
2-1 Yamada-oka Suita Osaka, 565-0871, Japan
kondo@see.eng.osaka-u.ac.jp

In order to conduct the water tank experiment that resembles the Katmandu valley, the dominant dimensionless parameters of both the flow field and the dispersion field were extracted by the numerical simulation. The dimensionless parameters in both atmospheric stability and instability condition were defined by the ratio of the mountain height to the mixing height and to the inversion height, respectively. The water tank experiment based on these dimensionless parameters of the Katmandu valley agreed with the numerical simulation reasonably. This result suggested that these dimensionless parameters can be applicable for the flow and dispersion phenomenon in the valley.

Key words: atmospheric instability, atmospheric stability, mixing height, inversion height, water tank experiment, numerical simulation, Katmandu valley

1. Introduction

Meteorological Phenomenon in meso scale are strongly influenced by heating and cooling of the ground surface depending on the geophysical feature or the landuse, and peculiar local air pollution phenomenon are brought by them. Though the physical approaches of air pollution phenomena are usually made by the numerical simulations, there are several researches on them by water tank model[1),2)].

Ueda[3)] reproduced land and sea breezes, and Chen[4)] reproduced mountain and valley winds. Both researches proposed the dimensionless parameters governing the local circulations. Author[5),6)] measured air pollution in Kathmandu valley and reported that air pollution in Kathmandu valley was strongly related to atmospheric stability. In this study, the dimensionless parameters for reproducing air pollution phenomena occurring in a valley were examined by the numerical simulation and air pollution phenomenon in Kathmandu valley were visualized by water tank experiment designed from the dimensionless parameters.

2. Numerical model in a valley

To design a water tank experiment in the Kathmandu valley, dimensionless parameters governing air pollution in a valley were extracted by the numerical simulation.

2.1. Basic equations

To simplify and generalize the phenomena, a two-dimensional and laminar model was adopted. The basic equations with Boussinesq approximation are

$$\frac{du}{dt} = -\frac{1}{\rho}\frac{\partial p'}{\partial x} + \nu\left(\frac{\partial^2 u}{\partial x^2} + \frac{\partial^2 u}{\partial z^2}\right) \quad (1)$$

$$\frac{dw}{dt} = -\frac{1}{\rho}\frac{\partial p'}{\partial z} + \beta T' g + \nu\left(\frac{\partial^2 w}{\partial x^2} + \frac{\partial^2 w}{\partial z^2}\right) \quad (2)$$

$$\frac{\partial u}{\partial x} + \frac{\partial w}{\partial z} = 0 \quad (3)$$

$$\frac{dT}{dt} = \kappa\left(\frac{\partial^2 T}{\partial x^2} + \frac{\partial^2 T}{\partial z^2}\right) \quad (4)$$

,where u, v, T, p are horizontal wind component, vertical wind component, temperature and pressure. ρ, ν, κ are density, viscous coefficient and thermal diffusivity of water. β, g are thermal expansion coefficient and gravity acceleration.

2.2 Calculation domain

The left side of a valley shown in Fig.1 is the calculation domain. The domain height is H (20cm). The slope height and width are H_b (2.5cm) and L_b (10cm), respectively. The width in the outside of the slop is L_m . The width in the inside of the slop is L_p . The geophysical feature of valley was expressed by

$$R_{bp} = \frac{H_b}{L_p} \quad (5)$$

The numerical simulations were carried out for $R_{bp} = 0.15$ and for $R_{bp} = 0.019$, which were corresponded with the deep valley and the shallow valley, respectively.

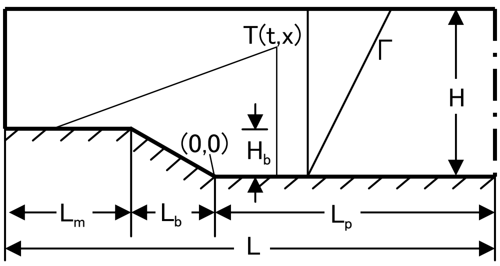

Fig.1 Calculation domain

2.2 Initial condition and boundary condition

The temperature gradient Γ was set as the initial condition. The surface temperature was periodically varied by the equation (6).

$$T(t,x) = k \sin\left(\frac{2\pi t}{t_p}\right) + T_0 + \Gamma z(x) \tag{6}$$

where,

$$z(x) = \begin{cases} 0 & (0 \le x) \\ -\dfrac{H_b}{L_b} x & (-L_b \le x < 0) \\ H_b & (x < -L_b) \end{cases} \tag{7}$$

k is the amplitude of temperature, t_p is the periodic time and T_0 is the initial temperature on the surface (standard temperature). The time to the maximum temperature $T_0 + T'_{\max}$ from standard temperature and the time the minimum temperature $T_0 - T'_{\min}$ from standard temperature was defined as t_c and t_d , respectively (see Fig.2).

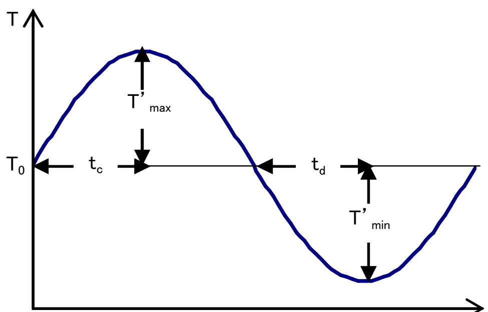

Fig.2 Time variation of surface temperature

The calculation was performed during 4 periodic times and the constant contamination q was continuously emitted from the inside surface of the slope after 2 periodic times. The adiabatic conditions were set at the left lateral boundary and at the top boundary. The symmetric conditions were set at the right lateral boundary.

3. Dimensionless parameters governing air pollution

3.1 dimensionless parameters in atmospheric instability

Chen[4] proposed the dimensionless parameter defined by

$$Gc = \frac{H_c}{H_b} \tag{8}$$

where H_c is the theoretic height that the air mass on the surface with temperature of $T_0 + T'_{\max}$ raises adiabatically and is defined by

$$Hc = \frac{T'_{\max}}{\Gamma} \tag{9}$$

H_c is the maximum value of the mixing height at daytime and is strongly related to air pollution at daytime.

The time variation of the simulated dimensionless concentration and the simulated dimensionless mixing height is shown in Fig.3 at the condition of $R_{bp} = 0.019$ and $G_c = 2$.

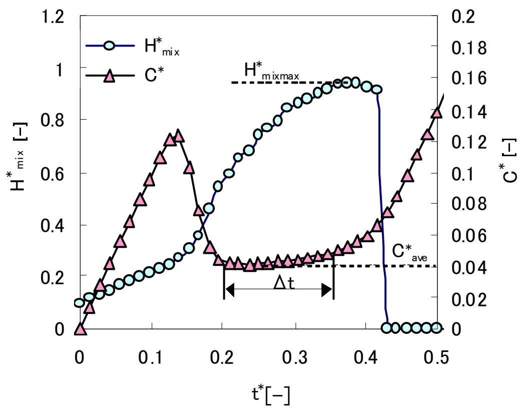

Fig.3 Time variation of mixing height and concentration

The dimensionless mixing height, the dimensionless time and the dimensionless concentration are defined by

$$H^* = \frac{H}{H_b} \tag{10}$$

$$t^* = \frac{t}{t_p} \tag{11}$$

$$C^* = \frac{C}{q \cdot t_p} \tag{12}$$

The averaged low concentration was considered as dimensionless parameter at daytime. The averaged time was defined by

$$\left|\frac{dc}{dt}\right| \le 0.1q \qquad (13)$$

At the condition of $R_{bp} = 0.15$ and $R_{bp} = 0.019$, the maximum mixing height and the averaged low concentration were calculated for the change of G_c. Figure 4 shows the relation between Chen's dimensionless parameter and the dimensionless maximum mixing height and the dimensionless averaged low concentration. It was shown that the dimensionless maximum mixing height and the dimensionless averaged low concentration were the monotonous function of G_c. These results mean that at the range $0.8 \le G_c \le 4.0$, air pollution phenomena at daytime were governed by only Chen's dimensionless parameter G_c.

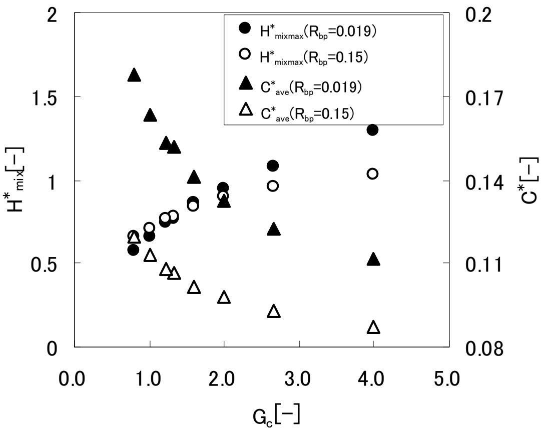

Fig.4 Relationship between mixing height H^*_{mixmax}, average concentration C^*_{ave} and dimensionless parameter G_c

3.2 dimensionless parameters in atmospheric stability

Chen[4] proposed the dimensionless parameter defined by

$$G_d = \frac{H_d}{H_b} \qquad (14)$$

where H_d means the maximum height of cool pond generated in nighttime and is defined by

$$H_d = \sqrt{kt_d} \qquad (15)$$

The time variation of the simulated dimensionless concentration and the simulated dimensionless height of cool pond is shown in Fig.5 at the condition of $R_{bp} = 0.019$ and $G_d = 0.2$

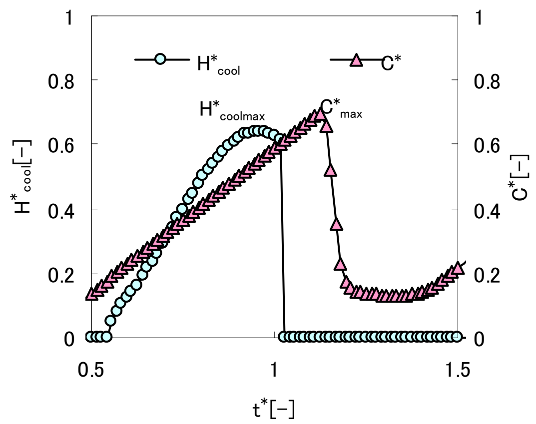

Fig5.Time variation of stable layer height and concentration

At the condition of $R_{bp} = 0.15$ and $R_{bp} = 0.019$, the maximum height of cool pond and the maximum concentration were calculated for the change of G_d. Figure 6 shows the relation between Chen's dimensionless parameter and the dimensionless maximum height of cool pond and the dimensionless maximum concentration. It was shown that the dimensionless maximum height of cool pond and the dimensionless maximum concentration were the monotonous function of G_d. These results mean that at the range $0.1 \le G_d \le 0.3$, air pollution phenomena at nighttime were governed by only Chen's dimensionless parameter G_d.

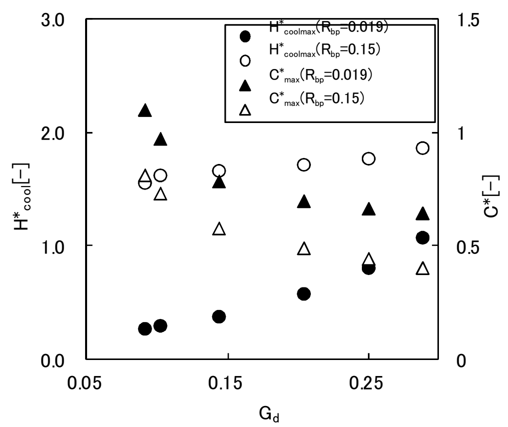

Fig6. Relationship between maximum stable layer height $H^*_{coolmax}$, maximum concentration C^*_{max} and dimensionless parameter G_d

4. Water tank experiment in Kathmandu valley

4.1. Experimental apparatus

The outline of the experimental apparatus is shown in Fig. 7 and the piping system is shown in Fig.8. The water tank apparatus was made from acrylic board and consisted of the top tank and the bottom tank. The top tank corresponded to atmosphere in Kathmandu valley and the bottom tank was used for temperature control of the ground surface by circulating hot water or cold water.

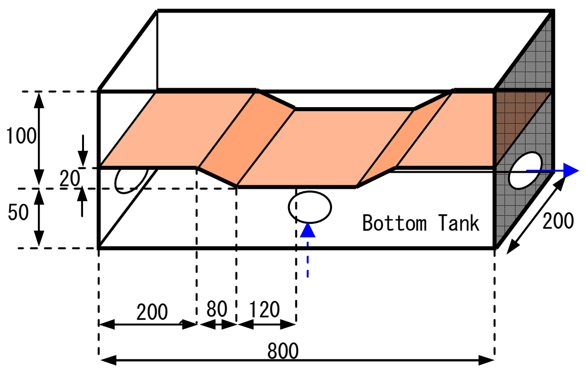

Fig.7 Outline of water tank experiment

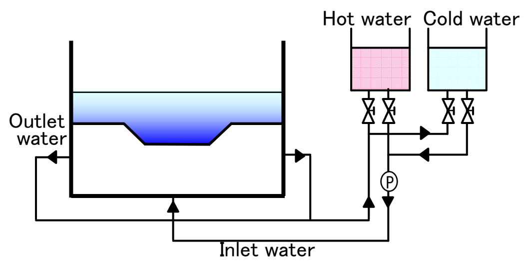

Fig.8 Outline of piping system

4.2. Experimental method

The surface temperature was changed according to the temperature variation in winter Kathmandu valley. In the experiment, the periodic time of 4 minutes was adopted as shown in Fig.9.

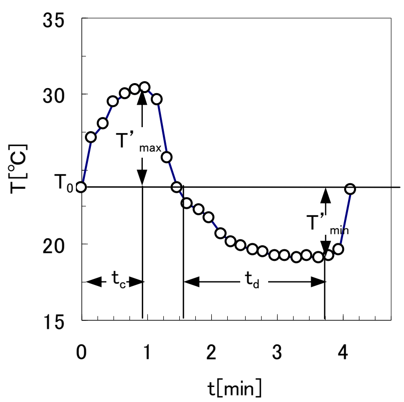

Fig.9 Surface temperature control in water tank experiment

4.3. Dimensionless parameter in water tank experiment

The values used in the water tank experiment and the values corresponded in Kathmandu valley are shown in Table 1. The dimensionless parameters in atmospheric instability and in atmospheric stability are shown in Table 2. The values of G_c and G_d in the water tank experiment and in Kathmandu valley were almost same. It is thought that this design in the water tank experiment could simulate air pollution phenomena in Kathmandu valley.

Table 1 Parameters values

Parameter	Experiment	Kathmandu valley
H_b	2.0 cm	1150 m
L_b	8.0 cm	4600 m
L_p	12.0cm	6750m
t_c	62 s	$1.26(10)^4$ s
t_d	104 s	$4.14(10)^4$ s
T'_{max}	6.6 ℃	8.4 ℃
T'_{min}	4.6 ℃	8.4 ℃
Γ_α, Γ	$3.57(10)^{-1}$ cm^2/kg	0.005 K/m
ν , ν_c	$10^{-2} cm^2s^{-1}$	$1\ m^2s^{-1}$
κ ,κ_{Te}	$1.4(10)^{-3} cm^2s^{-1}$	$1\ m^2s^{-1}$
β	$2.10(10)^{-4}K^{-1}$	-
H	7.0cm	-

Table 2 Dimensionless parameters values

Parameter	Experiment	Kathmandu valley
H_c	3.88cm	1680m
H_d	0.38cm	203m
G_c	1.94	1.46
G_d	0.193	0.177
R_{bp}	0.167	0.170

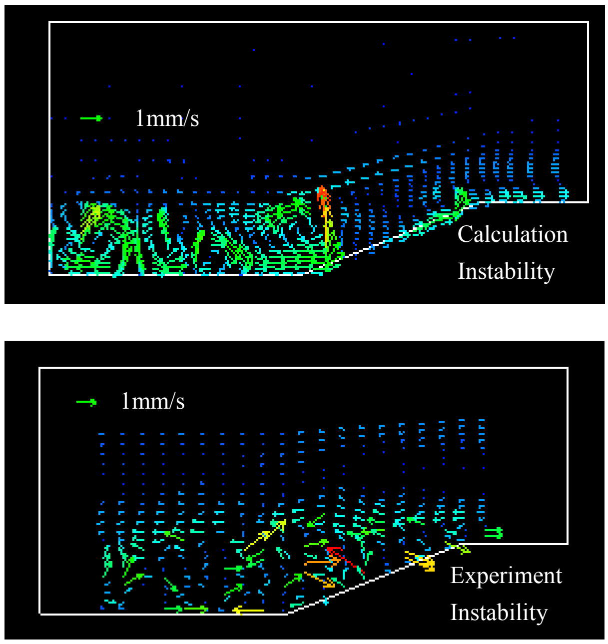

Fig.10 Flow vectors in instability

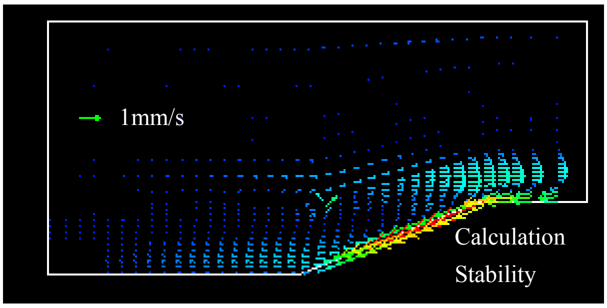

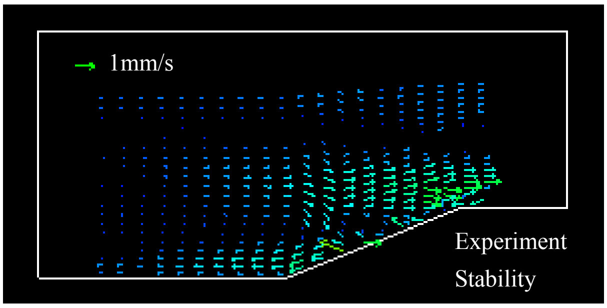

Fig.11 Flow vectors in stability

4.4. Flow in water tank experiment

The flow vectors in the water tank by particle image velocimetry[7] and in the numerical simulation were shown in Fig.10 and Fig.11. The vertical temperature distributions in instability and in stability were shown in Fig.12.

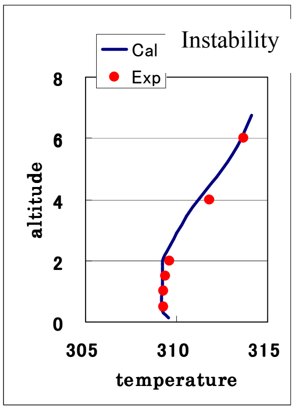

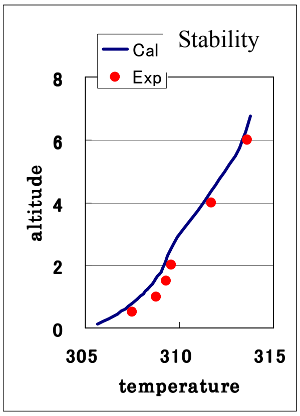

Fig.12 Temperature in instability and in stability

The maximum mixing height and the maximum height of cool pond in the water tank experiment reproduced the calculated results.

5. Conclusions

In this study, the dominant dimensionless parameters of both the flow field and the dispersion field were extracted by the numerical simulation. It was found that the dimensionless parameters proposed by Chen were useful for air pollution phenomena in a valley. The water tank experiment was designed by using these dimensionless parameters. The flow vectors and the vertical temperature distributions in the water tank experiment could reproduce the calculated results.

References

1) Mitsumoto,S., H. Ueda and H. Ozoe: A Laboratory Experiment on the Dynamics of the Land and Sea breeze, *J. Atmos. Sci*., **40**, (1983), 1228-1240

2) A.Kondo, A. Kaga, Y. Inoue, K.Yamaguchi, and H.W. Lee, Analysis of sea and land breezes in a water tank experiment and numerical simulation and influence of its flow fields on mass diffusion, Soc. Atmospheric Environment in Japan, **35**-5, (2000), 355-367 (Japanease).

3) H. Ueda: Effects of External Parameters on the Flow Field in the Coastal Region-A Linear Model-, *J. Climate and Appl. Meteor*., **22**, (1983), 312-321

4) Rui-Rong Chen, Neil S. Berman, Don L. Boyer and Harindra J. S. Fernando: Physical Model of Diurnal Heating in the Vicinity of a Two-Dimensional Ridge, *J.of Atmos. Sci*., **53**-1, (1996), 62-85.

5) A. Kondo: Comparison of field observation with water tank experiment on air pollution concentration in Kathmandu valley, Air Pollution X(Segovia, Spain), (2002), 493-502

6) KONDO Akira, KAGA Akikazu1, IMAMURA Kiyoshi, INOUE Yoshio, SUGISAWA Masahiko, SHRESTHA Manohar Lal, SAPKOTA Balkrishan, Investigation of air pollution concentration in Kathmandu valley during winter season, *Journal of Environmental Sciences*、**17**-6, (2005), 1009－1013

7) A. Kaga, Y. Inoueand K. Yamaguchi: Pattern Tracking Algorithms Using Successive Abandonment, *J of Flow Visualization and Image Processing*, **1**, (1993), 1, 283-296